Fast vortex motion and filamentary phase separation in high-T_c thin films

H. Yan, J. Jung,* and H. Darhmaoui†
Department of Physics, University of Alberta, Edmonton, Alberta, Canada T6G 2J1

Z. F. Ren‡ and J. H. Wang
Department of Chemistry, State University of New York at Buffalo, Buffalo, New York 14260-3000

W.-K. Kwok
Materials Science Division, Argonne National Laboratory, Argonne, Illinois 64039
(Received 18 May 1999; revised manuscript received 10 January 2000)

We investigated the temperature dependence of the normalized logarithmic relaxation rate $S(T)$ and the corresponding temperature dependence of the critical current $I_c(T)$ in high-T_c thin films (YBCO-123, TlBCCO-2212, -2223, and -2201, and Bi-2212). Experiments have been performed using persistent critical currents flowing in the *a-b* planes of ring-shaped samples. The magnitude of I_c and the relaxation rate have been extracted from the measurement of the self-field of the current. The results revealed a relationship between $I_c(T)$ and $S(T)$. $I_c(T)$ in YBCO is a superposition of two universal components: an underdoped Ginzburg-Landau- (GL-) like one with $I_c(T) \propto (T_c - T)^{3/2}$ and T_c between 40 and 60 K, and an Ambegaokar-Baratoff-like one close to an optimum doping. The results revealed that when the amount of the GL-like phase increases above a certain threshold value, a peak appears in $S(T)$ at temperatures of 20–30 K, and its height gradually increases with the magnitude of I_c at 10 K for this phase. We discuss similarities between these results and those reported for YBCO crystals with columnar defects. The presence of two maxima in $S(T)$ have been observed for TlBCCO films that are composed of three different phases, at temperatures close to T_c of two underdoped components. The studies imply that the filamentary phase separation on a nanometer scale level in the *a-b* planes is responsible for the changes in vortex dynamics.

I. INTRODUCTION

An unusual temperature dependence of the normalized logarithmic relaxation rate $S(T) = d \ln J / d \ln t$ for the motion of magnetic flux in high-temperature superconductors was reported very early by a few research groups during routine measurements of magnetization. These studies revealed a single- or a double-peak structure in $S(T)$ for many samples. A low-temperature peak at a temperature range of about 20–40 K has been observed more frequently than a double-peak feature with peaks at temperatures of about 20 and 60 K. Some samples did not exhibit any peaks except a plateau at low temperature and an upturn of S with an increasing temperature close to T_c. The presence of peaks in $S(T)$ has been reported for $YBa_2Cu_3O_{7-\delta}$ (YBCO) and $Bi_2Sr_2CaCu_2O_8$ (BSCCO) single crystals, YBCO thin films, and YBCO grain-oriented and polycrystalline samples.

Very early studies of $S(T)$, performed by Tuominen *et al.*,[1,2] revealed two peaks in $S(T)$ for unirradiated BSCCO crystals, during the measurement of longitudinal and transverse components of remnant magnetization.[1] For a magnetic field B (500 G) applied parallel to the c axis, $S(T)$ of a longitudinal component displayed two peaks, a low-temperature peak at 23 K, of magnitude of about 0.14, and a high-temperature peak at 60 K, of magnitude of about 0.05. It has been found that a low-temperature peak has been shifted to low temperature and its magnitude has been reduced with an increasing orientation angle θ between B and the c axis. A high-temperature peak, on the other hand, exhibited an increase in the magnitude with an increasing θ, without any change in the peak's temperature. Related measurements of $S(T)$ in unirradiated YBCO single crystals by the same group[3] displayed a single peak at 40 K of magnitude of 0.12. $S(T)$ of grain-oriented (unirradiated) YBCCO has been observed to include a peak at a temperature of about 30 K.[4] It has been detected[5] that an increasing applied magnetic field has been responsible for a shift of the peak to lower temperatures and a reduction of the peak's magnitude. Magnetic relaxation studies on YBCO thin films[6,7] revealed a peak of $S(T)$ at about 50–60 K; however, Goodyear *et al.*[7] pointed out that the temperature dependence of S is affected by the temperature of thin film growth as well as that of thin film annealing at a constant pressure of oxygen. A maximum of $S(T)$ as high as 0.1 has been also seen in ceramic granular samples of YBCO at temperatures between 20 and 40 K.[8,9] Replacement of yttrium with praseodymium in ceramic $Y_{1-x}Pr_xBa_2Cu_3O_{7-\delta}$ has been shown to generate two peaks in $S(T)$, which have been observed to shift to low temperature with an increasing x (Ref. 10). However, the measurements of $S(T)$ in a number of unirradiated and proton-irradiated YBCO crystals[11–13] revealed no peaks, but an increase of $S(T)$ with temperature or a plateau of $S(T)$ over a temperature range about 20–50 K, followed by a gradual increase of S at higher temperatures. An irradiation of YBCO crystals with gold or tin ions, in order to produce columnar defects, led to a dramatic modification of the temperature dependence of the magnetic relaxation rates.[14–17] The data have been recorded for magnetic fields parallel to defects over a range of 0.5–4.0 T and displayed a peak in $S(T)$. The maximum has been observed to shift from about 36 K at 0.5

 ©2000 The American Physical Society

T to low temperatures and its magnitude to decrease from a value of 0.1 at 0.5 T with an increasing magnetic field. This behavior is strikingly similar to that of unirradiated samples of grain-oriented YBCO (Ref. 5). A recent report on $S(T)$ in a field of 0.5 T in a proton-irradiated polycrystalline $HgBa_2Ca_2Cu_3O_{6+\delta}$ compound[18] demonstrated the presence of a peak at 60 K. Studies of $S(T)$ in irradiated samples have generated a lot of interest in an attempt to provide efficient pinning sites for magnetic flux lines in high-temperature superconductors.

One of the first theoretical explanations of the peaks in $S(T)$ has been provided by Hagen and Griessen[19] who interpreted the experimental data in terms of the distribution of activation energies in a sample, using an inversion procedure. Recently, a low-temperature maximum $S(T)$ in irradiated crystals of YBCO has been interpreted by Thompson *et al.*[14] on the basis of collective pinning theory as due to a change in the form of the vortex dynamics, i.e., from a variable-range vortex hopping at low temperature to a collective pinning by columnar defects at higher temperatures.

Our interest in the behavior of $S(T)$ has been stimulated by the striking similarity of the peaks in $S(T)$ and its magnetic field dependence observed in irradiated samples to that seen in unirradiated ones.[5,14] Although it appears that the dominant vortex pins are columnar defects in samples irradiated with heavy ions, little is known about the nature of the pinning sites that are responsible for the maxima of $S(T)$ in unirradiated samples.

We present experimental results of the measurements of the normalized logarithmic relaxation rate S as a function of temperature in unirradiated YBCO and Tl-Ba-Ca-Cu-O (TBCCO) thin films. These data have been compared with a temperature dependence of the critical current density $J_c(T)$. High-resolution transmission electron microscopy (HRTEM) studies by Etheridge at Cambridge University[20] revealed the presence of nanodomains (approximately 2 nm in size) in the copper-oxygen planes of an optimally doped YBCO sample with the domain walls oriented at an angle approximately 45° to the *a-b* axes. The nanodomains are correlated along the *c* axis. According to Etheridge, the nanodomains are of structural origin and formed in a struggle to relieve internal stresses in the *a-b* planes. The spacing between conventional twin boundaries in the same material was found to be approximately 50–100 nm.

Since the nanodomain size a_0 is of the order of the Ginzburg-Landau coherence length ξ_{GL}, one would expect the properties of a superconductor to be governed by the nanodomain structure (nanodomain walls) at low temperatures where $\xi_{GL}(T)<a_0$ [see Fig. 1(a)]. At higher temperatures where $\xi_{GL}(T)>a_0$, the superconducting properties could be treated as those of a continuous medium. A temperature T^* at which $\xi_{GL}(T^*)=a_0$ separates these two regimes. Clem *et al.*[21] used this approach in order to explain the temperature dependence of the critical current density in a nonogranular NbN thin film. At low temperatures where $\xi_{GL}(T)<a_0$, the critical current I_c is governed by the intergrain Josephson junctions and its temperature dependence has the Ambegaokar-Baratoff (AB) character. Close to T_c where $\xi_{GL}(T)>a_0$, the current does not ''see'' the junctions and the temperature dependence of I_c is governed by the suppression of the order parameter. At these temperatures (i.e., at $T>T^*\cong 0.85T_c$), the superconductor behaves like a continuous medium and $I_c(T)$ is described by Ginzburg-Landau (GL) theory $[I_c(T)\propto(T_c-T)^{3/2}]$. An Ambegaokar-Baratoff $I_c(T)$, with a crossover to a Ginzburg-Landau behavior at temperatures above $T^*\cong 0.85T_c$, has been also observed in optimally doped YBCO thin films.[22,23] Figure 1(d) shows an example of this behavior; the data (solid triangles) together with a theoretical fit based on Clem's model of $I_c(T)$ in a nanogranular superconductor. Fitting to the data has been achieved by varying the parameter ε_0, which is a coupling constant proportional to the ratio of the average Josephson coupling energy of the intergrain junctions to the superconducting condensation energy of a grain. The curve marked *A-B* represents $[I_c(T)]^{2/3}$ of a superconductor with a single Josephson junction. Oxygen depletion leads to a reduction in T_c and a dramatic change in the temperature dependence of I_c, which becomes that of a Ginzburg-Landau[22] with $I_c(T)\propto(T_c-T)^{3/2}$ [see Fig. 1(d), solid squares]. A GL dependence of $I_c(T)$ has been also observed by Jones *et al.*[24] who measured $I_c(T)$ *in situ* in oxygen-depleted YBCO thin films. Figure 1(b) shows a schematic picture of a nanodomain structure where most of the cells have been oxygen depleted. In this case the critical current is no longer determined by the Josephson junctions, but by the suppression of the order parameter inside the cells. This could mean that one is allowed to extend the Ginzburg-Landau solutions for $I_c(T)$ (which are valid close to T_c in an optimally doped superconductor) down to low temperatures.[25]

If the superconductor is a mixture of optimally doped and underdoped phases, the nanodomain structure could look like a ''disordered chessboard'' [see Fig. 1(c)]. In this case the flow of the current is a percolative process. The critical current that flows entirely through optimally doped cells [white squares in Fig. 1(c)] is determined by the Josephson junctions in the nanoarray and its temperature dependence is the one that has been described by the Clem's model [solid triangles in Fig. 1(d)]. On the other hand, the critical current that crosses underdoped regions [shaded dark squares in Fig. 1(c)] is determined by the suppression of the order parameter and T_c in underdoped cells, and its temperature dependence is given by GL theory [solid squares in Fig. 1(d)]. The total critical current that flows through disordered nanostructures (and its self-magnetic field) is a superposition of these two critical currents. The temperature dependence of the critical current in this case is like that shown in Fig. 1(e), which is typical of most YBCO films studied. The ratio of $I_c(T)$ that is governed by an underdoped component [GL dependence, dashed straight line on $(I_c)^{2/3}$ versus temperature graph in Fig. 1(e)] to $I_c(T)$ which is determined by an optimally doped component [AB dependence (Clem's model), solid triangles on $(I_c)^{2/3}$ versus temperature graph in Fig. 1(e)] is sample dependent and could vary from zero to infinity. This is due to the fact that there is an infinite number of possibilities to arrange disorder in a ''disordered chessboard'' as shown in Fig. 1(c).

We found the correlation between this ratio and the height of the low-temperature peak in the temperature dependence of the magnetic relaxation rate $S(T)$. These findings imply that the electrical transport and magnetic properties of high-T_c thin films are governed by the filamentary phase separation (at the nanoscopic level) in the copper-oxygen planes.

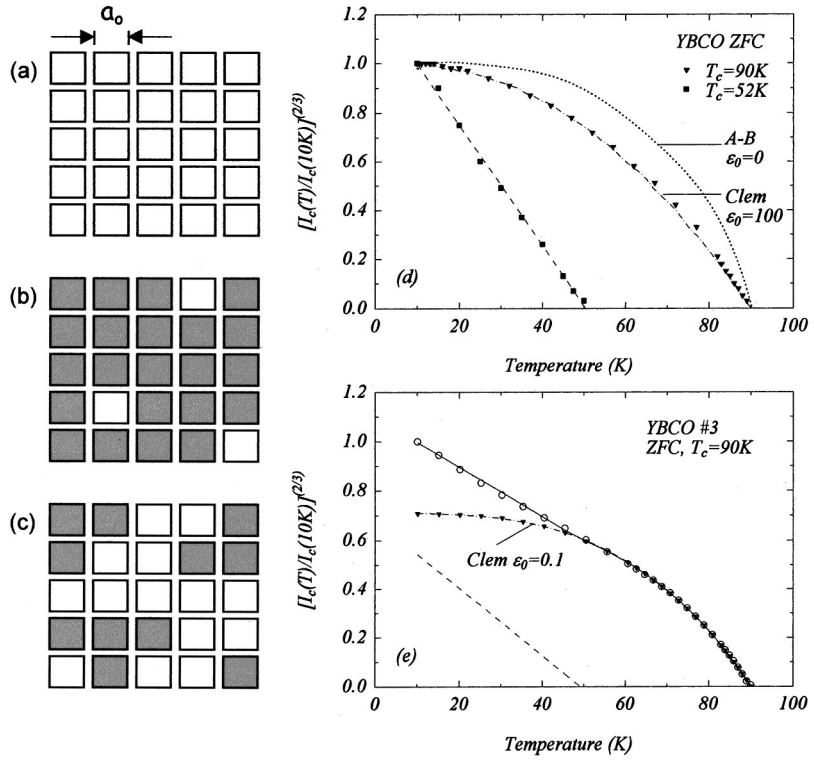

FIG. 1. (a), (b), (c) Schematic representation of nanostructures in the copper-oxygen planes. The *a* and *b* axes are approximately 45° relative to the domain walls (see Ref. 20). The nanodomain size a_0 is approximately a few nanometers. An optimally doped superconductor has nanostructures as in (a), where the critical current I_c is governed by the Josephson nanoarray. The temperature dependence of I_c is that of an Ambegaokar-Baratoff one at low temperatures and that of a Ginzburg-Landau one above approximately $0.85T_c$ as described by the Clem's model (Ref. 21) [see solid triangles in (d)]. The dotted line shows $I_c(T)$ of a single Josephson junction (pure Ambegaokar-Baratoff dependence). An underdoped superconductor is shown in (b), where I_c is governed by the suppression of the order parameter in the nanodomain. $I_c(T)$ is that of Ginzburg-Landau dependence [see the solid squares in (d)]. When a superconductor is a mixture of optimally doped and underdoped phases, its nanostructure is described schematically by a ''disordered chessboard'' shown in (c). In this case $I_c(T)$ is a superposition of two components shown in (d), i.e., an optimally doped one with an AB-like $I_c(T)$ (solid triangles) and an underdoped one with a GL-like $I_c(T)$ (solid squares and dashed line). A typical $I_c(T)$ of this type of a superconductor is presented in (e). The solid line is a fit to the experimental data (open circles), which is a superposition of the two components as mentioned above.

II. EXPERIMENTAL PROCEDURES

Investigations of $S(T)$ and its relationship to $J_c(T)$ have been performed for nine YBCO thin films, six TlBCCO films (of 2212 and 2223 composition), and underdoped TlBCO-2201 and BiSCCO-2212 films. Information on these films is listed in Table I, which includes T_c, film thickness, J_c at 10 and 77 K, deposition method, and a substrate. About a half of YBCO films have been manufactured using a pulsed laser deposition method at McMaster University, National Research Council in Ottawa, and IBM TJ Watson Research Center. The rest of the YBCO films have been produced with a rf and dc magnetron sputter-deposition method at the University of Alberta and Westinghouse STC. Tl- and Bi-based thin films have been deposited with a pulsed laser ablation method, followed by post-annealing, except magnetron-sputtered underdoped TlBCO (2201) film. These films came from CTF Systems, STI at Santa Barbara, and SUNY at Buffalo.

The measurements have been performed mostly on ring-shaped samples (of inner and outer diameters of 5.0 and 8.5 mm, respectively) with the *c* axis of the film directed along the ring's axis. The magnetic flux was introduced into the hole of the ring (which has been cooled below T_c in a zero field) by applying an external magnetic field, using a copper-wound solenoid, in the *c*-axis direction. A circulating persistent current was established in the ring after the external field was removed. The magnitude of the persistent current was determined from the axial component of the current's self-field using the Biot-Savart law. The measurement of the component of the self-field, perpendicular to the ring's plane, was done with a scanning axial Hall probe. Persistent current of the critical magnitude has been obtained when an increasing applied magnetic field produced a saturation of the current's self-field. This procedure allowed us to measure the dependence of the critical current on temperature and the time decay of the current from its critical value. Details of this technique have been reported in Refs. 22 and 23. The measurements have been performed over a temperature range between 10 K and T_c. An external magnetic field up to 1 kG was sufficient to generate critical currents over this temperature range in all samples. Two samples (see Table I) have been studied as a disk-shaped ones of 8.5 mm in diameter. In this case the critical current has been determined from the computer simulation of the axial profile (in the direction perpendicular to the disk plane) of the remnant magnetization at the saturation level. The profile and the critical current were calculated from the Biot-Savart equations by filling the disk with a large number of concentric

TABLE I. Composition, superconductiong transition temperature T_c, thickness, critical current density J_c, deposition method, and substrate used [(100) orientation] of high-T_c thin films that have been investigated during the course of these studies. PA denotes post-annealing. Sample YBCO No. 1A is YBCO No. 1B after irradiation with high-energy (1.4 GeV) uranium ions to obtain a matching field B_ϕ of 0.5 T.

Sample	Composition	T_c (K)	Thickness (nm)	J_c (A/cm^2) (10 K)	J_c (A/cm^2) (77 K)	Deposition method	Substrate
YBCO No. 1A	(123)	87	200	1.2×10^7	1.5×10^6	rf magnetron	$SrTiO_3$
YBCO No. 1B	(123)	89	200	1.0×10^7	1.1×10^6	rf magnetron	$SrTiO_3$
YBCO No. 2	(123)	87	280	6.5×10^6	2.4×10^5	rf magnetron	$SrTiO_3$
YBCO No. 3	(123)	90	500	1.1×10^7	1.5×10^6	dc magnetron	$LaAlO_3$
YBCO No. 4	(123)	91	200	1.8×10^7	1.7×10^6	Laser ablation	$LaAlO_3$
YBCO No. 5	(123)	87	250	4.0×10^6	2.0×10^5	Laser ablation	Sapphire
YBCO No. 6	(123)	87	120	2.3×10^7	7.1×10^5	rf magnetron	$LaAlO_3$
YBCO No. 7	(123)	90	300	1.5×10^7	1.7×10^6	Laser ablation	$LaAlO_3$
YBCO No. 8	(123)	90	100	3.3×10^7	2.8×10^6	Laser ablation	$SrTiO_3$
YBCO No. 9	(123)	89	250	2.8×10^7	2.6×10^6	Laser ablation	$LaAlO_3$
TBCCO No. 1	(2212)	99	500	8.8×10^5	4.0×10^4	Laser ablation+PA	$LaAlO_3$
TBCCO No. 2	(2212)	89	480	1.2×10^6	4.0×10^5	Laser ablation+PA	$LaAlO_3$
TBCCO No. 3	(2223)	101	500	2.4×10^6	2.4×10^5	Laser ablation+PA	$LaAlO_3$
TBCCO No. 4	(2212)	104	650	8.4×10^6	1.1×10^6	Laser ablation+PA	MgO
TBCCO No. 5	(2212)	103	650	8.4×10^6	9.5×10^5	Laser ablation+PA	MgO
TBCO No. 1 (disk)	(2201)	48	200	1.9×10^6	NA	Magnetron	$SrTiO_3$
BSCCO No. 1 (disk)	(2212)	60	500	1.6×10^6	NA	Laser ablation+PA	$LaAlO_3$

current loops. The time decay of a persistent current from the critical value has been measured over a time interval of 10–30 000 s (see Fig. 2). S has been determined using the data for times between 100 and 10 000 s, which is similar to the time window applied in Refs. 12, 15, and 18. In this time range, a magnetic relaxation is close to logarithmic as a function of time for all temperatures of the measurement. YBCO film Nos. 1 and 7 have been irradiated at ATLAS with a high dose of uranium and lead ions of energy 1.4 GeV, respectively. The ions produced columnar tracks along the c axis that were able to trap a magnetic field of 0.5 T.

III. EXPERIMENTAL RESULTS

Figures 3, 4, and 5 present experimental data for the temperature dependence of the critical current $I_c(T)$ and that of the normalized logarithmic relaxation rate $S(T)$, measured in YBCO thin films. $I_c(T)$ has been plotted as $(I_c)^{2/3}$ versus temperature in order to identify components in $I_c(T)$ that have a GL-like temperature dependence, i.e., $I_c(T)\propto(T_c-T)^{3/2}$. These components are represented by straight dashed lines in the $(I_c)^{2/3}$ vs temperature graphs. In fact, $[I_c(T)]^{2/3}$ is a superposition of two components: an underdoped GL-like component of T_c between 40 and 60 K and an AB-like one that is close to an optimum doping.

Solid lines in Figs. 3(a), 3(c), 3(e), 4(a), 4(c), 4(e), 5(a), 5(c), and 5(e) present a theoretical fit to the experimental data for $I_c(T)$. The fit represents a superposition of a GL-like $I_c(T)\propto(T_c-T)^{3/2}$ and an AB-like one obtained from Clem's model with a coupling constant ε_0 as the only fitting parameter. At a temperature of 10 K, the ratio of the current flowing through GL-like phase I_{GL} to that passing through an AB-like one I_{AB} is sample dependent. Therefore, Figs. 3(a), 3(c), 3(e), 4(a), 4(c), 4(e), 5(a), 5(c), and 5(e) are aligned in order to reflect an increasing contribution of I_{GL} (at 10 K) to the total current flowing in the sample. Figures 3(b), 3(d), 3(f), 4(b), 4(d), 4(f), 5(b), 5(d), and 5(f) show the corresponding temperature dependence of the normalized logarithmic relaxation rate $S(T)$. A low-temperature maximum in $S(T)$ develops at temperatures of about 25–30 K, when the ratio I_{GL} (10 K)/I_{AB} (10 K) exceeds 0.5. The height of the peak increases with an increasing ratio I_{GL}/I_{AB}. Figure 6 presents the dependence of the height ΔS of the maximum in $S(T)$ [i.e., $\Delta S\cong S(\text{peak})-S$ (10 K)] on I_{GL}/I_{AB} at 10 K. The

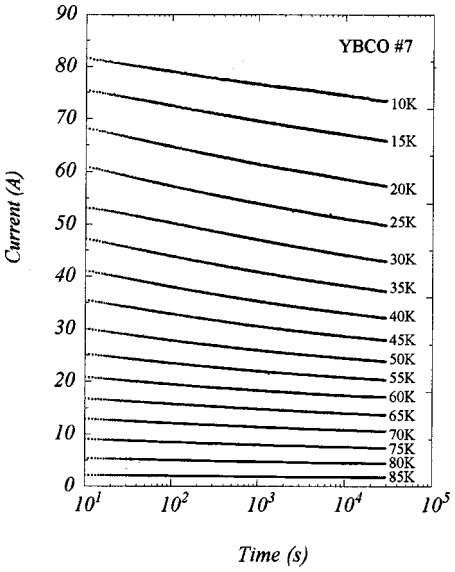

FIG. 2. Time decay of the persistent current (flowing in a ring of YBCO 7) from the critical value for temperatures between 10 and 85 K. The normalized logarithmic relaxation rate S has been calculated for a time range between 100 and 10 000 s.

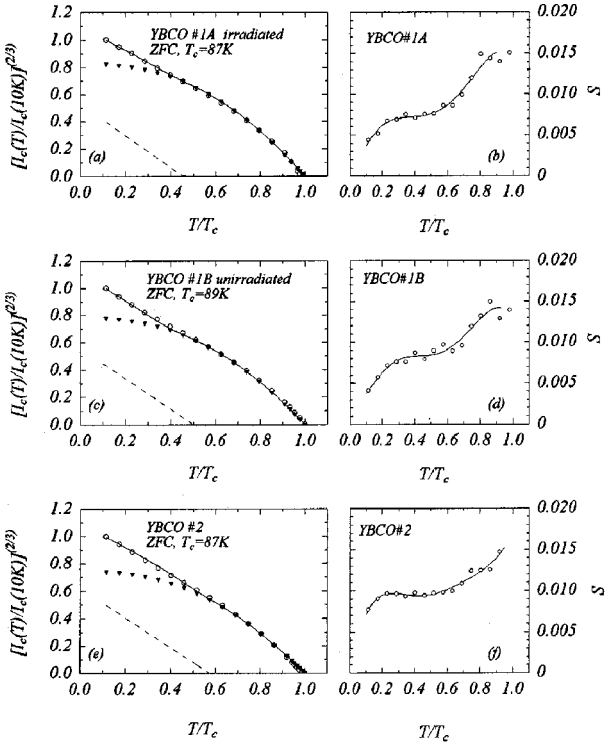

FIG. 3. The dependence of the critical current on the normalized temperature [plotted as $[I_c(T)/I_c(10\,\mathrm{K})]^{2/3}$ vs T/T_c in the figures on the left, (a), (c), and (e)] compared with the dependence of the relaxation rate S on temperature in the figures on the right, (b), (d), and (f), for YBCO ring-shaped films 1A, 1B, and 2. In (a), (c), and (e) the open circles mark the experimental data for $I_c(T)$. The solid line represents theoretical fit to the experimental data: they are the superposition of the GL-like dependence (dashed line) at low temperature and the AB-like dependence [Clem's model (solid triangles) with the coupling constant $\varepsilon_0=100$ for (a), (c), and (e)]. In (b), (d), and (f) the open circles mark the experimental data with the solid line as the guide for the eye. (a), (c), and (e) are aligned in order to reflect an increasing contribution of the GL-like component to the total critical current.

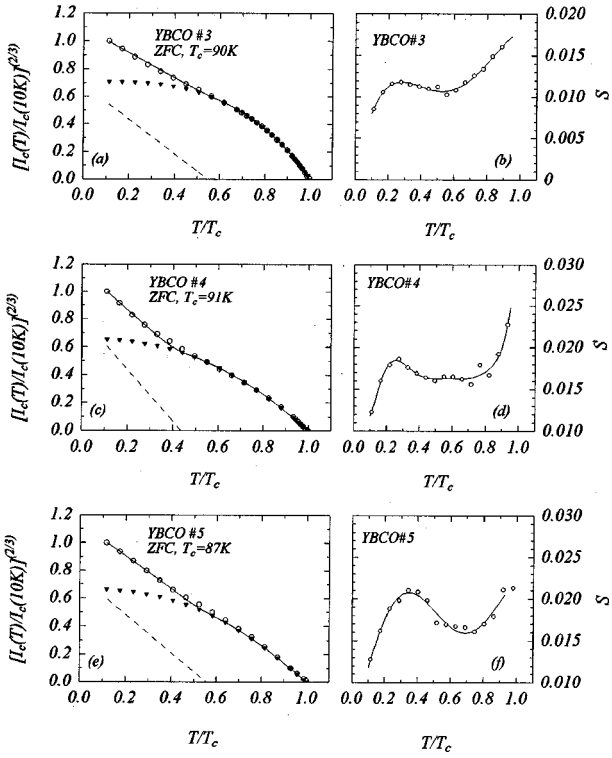

FIG. 4. The dependence of the critical current on the normalized temperature [plotted as $[I_c(T)/I_c(10\,\mathrm{K})]^{2/3}$ vs T/T_c in the figures on the left (a), (c) and (e)] compared with the dependence of the relaxation rate S on temperature in the figures on the right (b), (d), and (f), for YBCO ring-shaped films 3, 4, and 5. In (a), (c), and (e) the open circles mark the experimental data for $I_c(T)$. The solid line represents theoretical fit to the experimental data: they are the superposition of the GL-like dependence (dashed line) at low temperature and the AB-like dependence [Clem's model (solid triangles)] with the coupling constant $\varepsilon_0=0.1$ for (a) and $\varepsilon_0=100$ for (c) and (e).] (a), (c), and (e) are aligned in order to reflect an increasing contribution (higher than that for samples 1A, 1B, and 2) of the GL-like component to the total critical current. In (b), (d), and (f) the open circles mark the experimental data with the solid line as the guide for the eye.

rate of an increase of ΔS with $I_{\mathrm{GL}}/I_{\mathrm{AB}}$ depends on the magnitude of T_c of an underdoped GL-like component [see Figs. 3(a), 3(c), 3(e), 4(a), 4(c), 4(e), 5(a), 5(c), and 5(e)]. In fact, ΔS appears to be higher for samples whose GL-like components have the highest T_c of about 50–60 K. Figures 7(a), 7(c), 7(e) and 7(b), 7(d), 7(f) show $(I_c)^{2/3}$ versus T/T_c and S versus T/T_c, respectively, for underdoped Tl-Ba-Ca-Cu-O thin films of 2212 and 2223 compositions. The temperature dependence of the critical current in these films is dominated by a Ginzburg-Landau-like behavior. The underdoped GL components have superconducting transition temperatures close to T_c of the films, i.e., of the order of $(0.75-0.90)T_c$. The temperature dependence of the relaxation rate S in Fig. 7(b), 7(d), and 7(f) reveals that S increases gradually with temperature, reaching a maximum close to T_c. For Tl-2212 close to an optimum doping, $S(T)$ exhibits two maxima, one at low temperatures about $0.2T_c$ and the other of much higher magnitude close to T_c at $(0.75-0.80)T_c$ [see Figs. 8(b) and 9(b)]. The corresponding temperature dependence of $I_c^{2/3}$ shows the presence of three components: an underdoped GL-like one of $T_c=40-45\,\mathrm{K}$ and two AB-like components of different T_c [see Figs. 8(a), 8(c), 8(d) and 9(a), 9(c), 9(d)]. Two AB-like contributions to $I_c(T)$ suggest the presence of two different phases of Tl-Ba-Ca-Cu-O in the samples with the superconducting transition temperatures of 92.5 and 102 K for TBCCO No.4 and 87.5 and 102 K for TBCCO No. 5. Phases of lower T_c of 92.5 and 87.5 K have been identified as those of a different composition, namely, Tl-1212. Figure 10 presents the data for underdoped Tl-2201 and Bi-2212 thin films. $I_c(T)$ of these samples is characterized by a GL-like temperature dependence at low temperatures and $S(T)$ exhibits peaks at $0.4T_c$ and $0.65T_c$ for Tl- and Bi-based films, respectively.

IV. DISCUSSION

The experimental results, presented above, imply that the temperature dependence of the normalized logarithmic relaxation rate S is governed by the phase separation in the *a-b* planes of high-T_c thin films. For YBCO films we discovered a correlation between a low-temperature maximum in $S(T)$

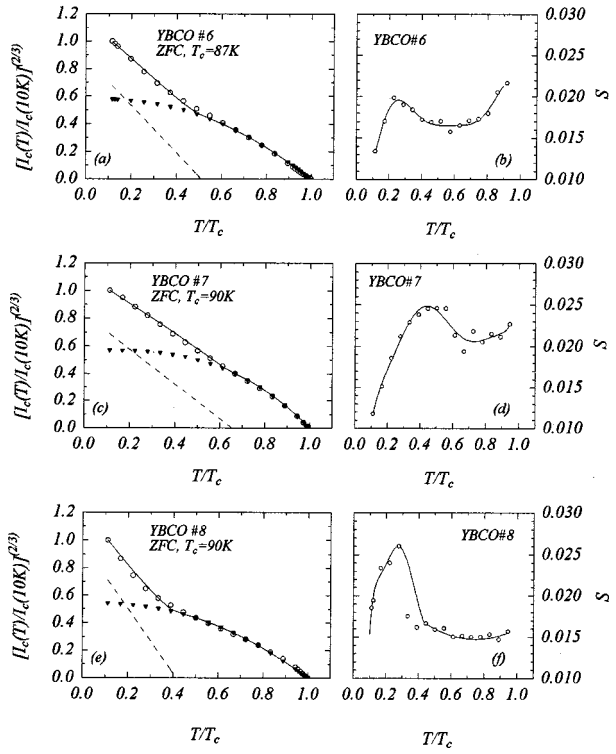

FIG. 5. The dependence of the critical current on the normalized temperature [plotted as $[I_c(T)/I_c(10\,\mathrm{K})]^{2/3}$ vs T/T_c in the figures on the left, (a), (c), and (e)] compared with the dependence of the relaxation rate S on temperature in the figures on the right, (b), (d), and (f), for YBCO ring-shaped films 6, 7, and 8. In (a), (c), and (e) the open circles mark the experimental data for $I_c(T)$: they are the superposition of the GL-like dependence (dashed line) at low temperature and the AB-like dependence [Clem's model (solid triangles) with the coupling constant $\varepsilon_0 = 100$ for (a), (c), and (e)]. (a), (c), and (e) are aligned in order to reflect an increasing contribution of the GL-like component (higher than that for samples 3, 4, and 5) to the total critical current. In (b), (d), and (f) the open circles mark the experimental data with the solid line as the guide for the eye.

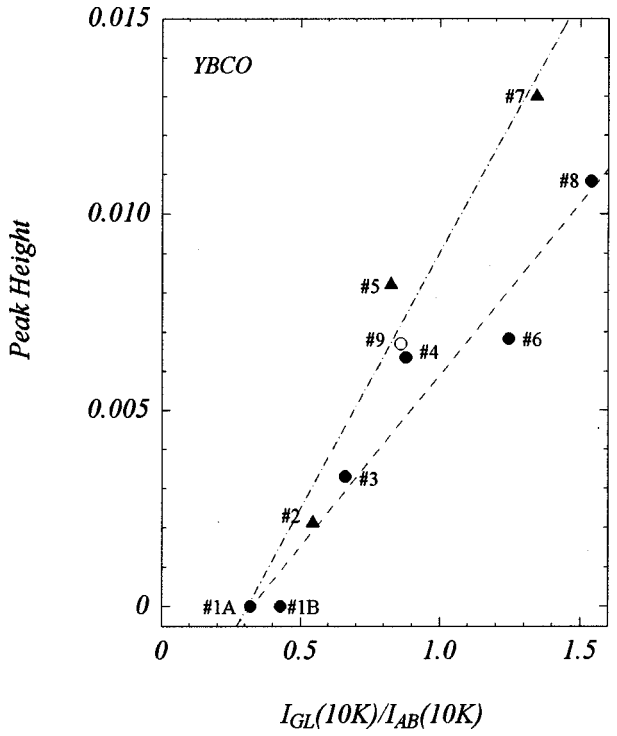

FIG. 6. The dependence of the height of the low-temperature peak in $S(T)$ which has been measured in YBCO thin films, approximately with respect to S at 10 K, on the ratio of the critical current flowing through a GL-like underdoped phase at 10 K to the corresponding one flowing through an AB-like phase. The rate of the increase in the peak's height with $I_{GL}(10\,\mathrm{K})/I_{AB}(10\,\mathrm{K})$ depends on T_c of the GL-like phase. Higher rates are observed for T_c over a range between 55 and 60 K (solid triangles) and the lower ones for T_c between 40 and 45 K (circles).

and the amount of the critical current flowing at low temperatures through an underdoped YBCO phase. The temperature dependence of this critical current is a GL-like one. The maximum of $S(T)$ is located at temperatures corresponding to a temperature range at which the underdoped YBCO phase exists (Figs. 3–5). A maximum in $S(T)$ at similar temperatures has also been observed in high-J_c Tl-2212 thin films that contain a underdoped phase of a GL-like $I_c(T)$ with T_c of about 20 K seen in Figs. 8 and 9. In fact, the same films exhibit a second maximum in $S(T)$ at higher temperatures. The critical current in these films is carried by three phases: therefore, this suggests that the second maximum is associated with a phase of higher T_c, namely, Tl-1212. The $I_c(T)$ of underdoped Tl-2212, Tl-2223, Tl-2201, and Bi-2212 films (Figs. 7 and 10) is dominated at low temperatures by a GL-like temperature dependence and $S(T)$ reveals a broad maximum. Close to T_c, $I_c(T)$ deviates from a GL-like temperature dependence. This implies the presence of a second phase which contributes to the critical current flowing in the sample. Using the same arguments that have been applied to YBCO thin films, a two-phase superconductor should exhibit a single maximum in $S(T)$, if the ratio of the critical current flowing through an underdoped GL-like phase at 10 K to that flowing through a second phase of higher T_c exceeds a certain value.

The experimental results suggest that the phase separation is responsible for the observed maxima in $S(T)$. $I_c(T)$ revealed that the current flows through two or three parallel ''channels'' (''filaments'') associated with the presence of two or three different superconducting phases. In YBCO films, there are two channels of the current flow [see the discussion of $I_c(T)$ in the Introduction]. The first one could be associated with an optimally doped AB-like phase, which forms continuous paths in the *a-b* plane. The other channel is dominated by an underdoped GL-like phase, which forms discontinuous paths or islands in the *a-b* planes of the films [see Fig. 1(c)]. It is important to realize that the ratio of the magnitudes of the critical current at 10 K, which flows through a low-T_c GL-like phase to that through a high-T_c AB-like one, is sample dependent. This ratio can be zero [pure AB-like case, solid triangles in Fig. 1(d)] or infinity [pure GL-like case, dashed line in Fig. 1(d)]. However, this is a mixture of both phases, which is responsible for the changes in vortex dynamics [see Figs. 1(c) and 1(e)]. In fact, there is an infinite number of possibilities for the ratio of I_c^{GL}/I_c^{AB} at 10 K. This agrees with the filamentary picture of high-T_c superconductors on a nanoscopic level, in which the amount of an underdoped phase and its T_c affect the relaxation of the persistent current.

The presence of a low-temperature maximum in $S(T)$ of

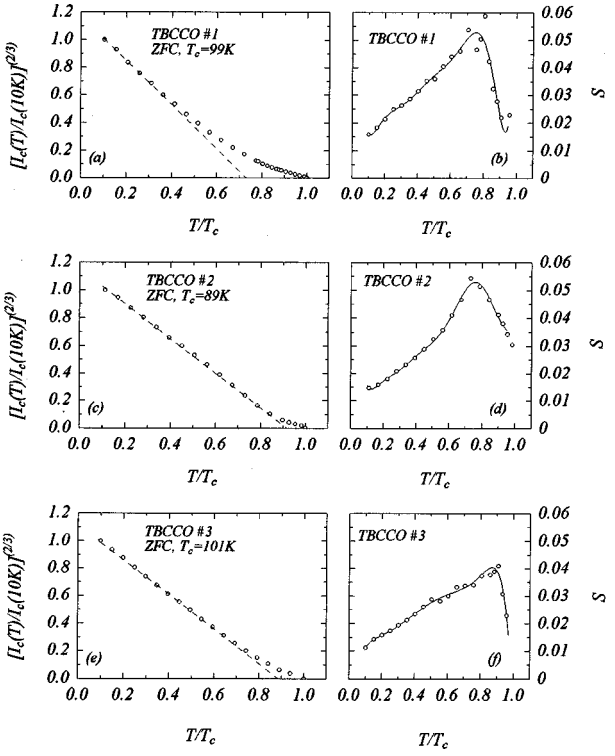

FIG. 7. The dependence of the critical current on the normalized temperature [plotted as $[I_c(T)/I_c(10\,\mathrm{K})]^{2/3}$ vs T/T_c in the figures on the left] compared with the dependence of the relaxation rate S on temperature in the figures on the right for underdoped TIBCCO films 1, 2 (2212 phase), and 3 (2223 phase). Note that $I_c(T)$ is dominated by an underdoped GL-like component at low temperature. A tail close to T_c implies the presence of an unidentified second component (phase).

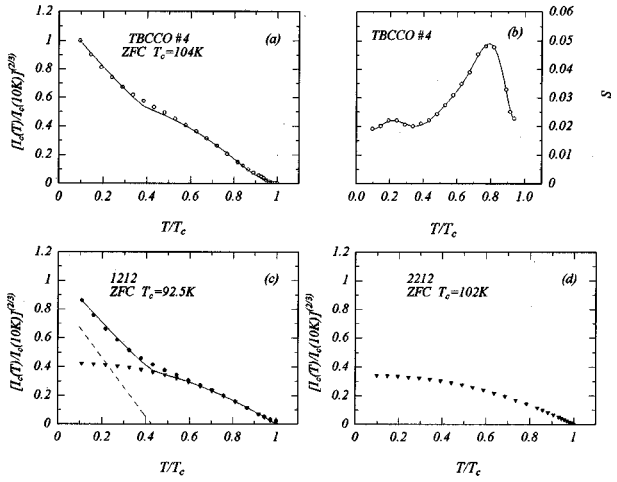

FIG. 8. The dependence of the critical current on the normalized temperature [plotted as $[I_c(T)/I_c(10\,\mathrm{K})]^{2/3}$ vs T/T_c in (a) on the left] compared with the dependence of the relaxation rate S on temperature in (b) on the right for TIBCCO (2212) ring-shaped film 4. In (a) the open circles mark the experimental data for $I_c(T)$. The solid line represents theoretical fit to the experimental data: they are the superposition of three different contributions to $I_c(T)$. Two of these contributions, which are associated with the presence of the 1212 phase, are shown in (c). They are an underdoped GL-like component (dashed line) and an AB-like component [Clem's model (solid triangles) with a coupling constant $\varepsilon_0=100$]. Note that two peaks in $S(T)$ are related to these two components. The third contribution is due to the 2212 phase of $T_c=102\,\mathrm{K}$, which exhibits an AB-like behavior [Clem's model (solid triangles) with a coupling constant $\varepsilon_0=100$] in (d).

irradiated samples with columnar defects[14] has been interpreted as a competition between two types of vortex dynamics. In the collective pinning theory[26] the relaxation rate S is given by

$$S=\frac{kT}{U_0(T)+\mu kT\ln(t/t_0)},$$

where t_0 is the logarithmic time scale that depends on a sample size, U_0 is the unperturbed pinning potential, and μ is the exponent in the power law dependence of the energy barrier on the current density. Starting from low temperatures U_0 is large, but decreases with an increasing temperature, leading to an increase of S with temperature.[14,27] A peak in $S(T)$ forms as a result of a crossover to a different vortex pinning regime. The exponent μ depends on the vortex dynamics at a certain temperature, magnetic field, and critical current density. If μ changes from a small value (e.g., $\mu=1/3$ for a variable-range vortex hopping) at low temperature to a larger one (e.g., $\mu=3/2$ for a collective creep of small flux bundles) at higher temperature, S will decrease with an increasing temperature and a maximum appears in $S(T)$.

We applied an idea of a crossover between two different regimes of vortex dynamics in order to interpret the data for unirradiated YBCO thin films that contain an underdoped phase of T_c between 40 and 60 K. We assume (in the same way as for irradiated samples) that S increases with temperature gradually, starting from low temperature (due to a gradual reduction of U_0 with an increasing temperature), and reaches a high value close to T_c. We expect similar behavior of $S(T)$ for both phases: an underdoped GL-like one and an AB-like one close to optimum doping. Therefore, in YBCO films an increase of S with temperature at low temperatures is dominated by an underdoped phase. The rise of $S(T)$ continues until the temperature is close to T_c of this phase. $S(T)$ reaches a maximum and then descends due to a reduction in the order parameter of the underdoped GL-like phase. According to Clem *et al.*[21] in the Ginzburg-Landau regime of the critical current close to T_c, one should expect current-induced gap suppression. Therefore, in the GL-like underdoped phase close to its T_c, the order parameter is reduced in the presence of the supercurrent, and subsequently it disappears above T_c. At temperatures above T_c of the underdoped phase, the superconductor is a mixture of a normal phase and a superconducting one whose $I_c(T)$ is characterized by an AB-like behavior. The experimental results show that the mechanism of vortex-dynamics-induced dissipation of the current depends on the amount of the GL-like underdoped phase and its T_c, which is sample dependent. Preliminary measurements of the magnetic penetration depth in the *a-b* planes YBCO thin films[28] revealed that the low-temperature part of the temperature dependence of the superfluid density $n_s(T)$ is affected by the ratio of the amount of an underdoped phase in a superconductor [with a GL-like $I_c(T)$] to that of an optimally doped one [with an

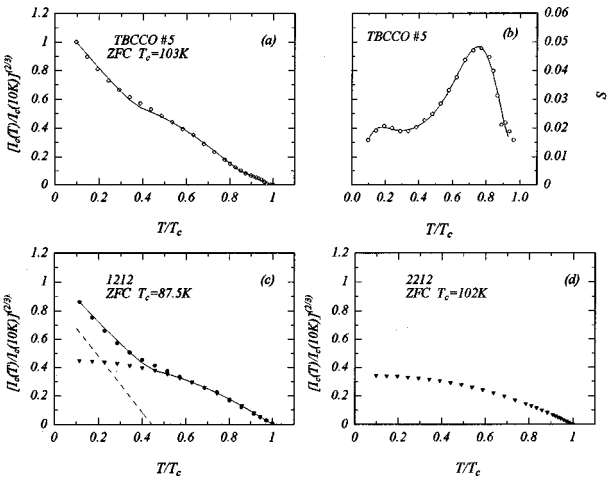

FIG. 9. The dependence of the critical current on the normalized temperature [plotted as $[I_c(T)/I_c(10\,\mathrm{K})]^{2/3}$ vs T/T_c in (a) on the left] compared with the dependence of the relaxation rate S on temperature in (b) on the right for TIBCCO (2212) ring-shaped film 5. In (a) the open circles mark the experimental data for $I_c(T)$. The solid line represents theoretical fit to the experimental data: they are the superposition of three different contributions to $I_c(T)$. Two of these contributions, which are associated with the presence of the 1212 phase, are shown in (c). They are an underdoped GL-like component (dashed line) and an AB-like component [Clem's model (solid triangles) with a coupling constant $\varepsilon_0=100$]. Note that two peaks in $S(T)$ are related to these two components. The third contribution is due to the 2212 phase of $T_c=102$ K, which exhibits an AB-like behavior [Clem's model (solid triangles) with a coupling constant $\varepsilon_0=100$] in (d).

AB-like $I_c(T)$]. Since the penetration depth $\lambda(T)$ and $n_s(T)$ do not depend on the energy barrier against motion of the magnetic flux, this experiment is an important confirmation that the temperature dependence of the critical current is

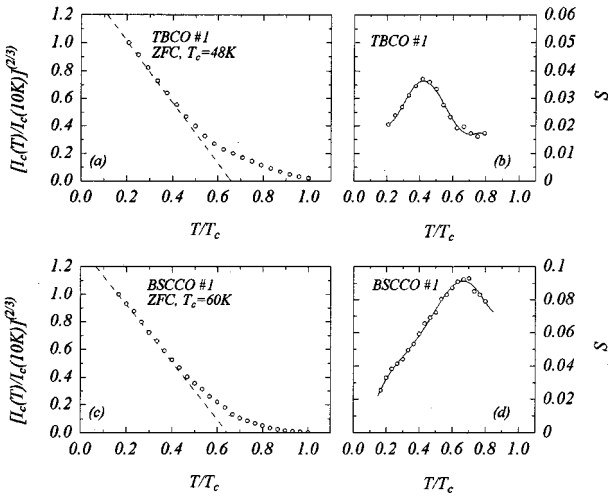

FIG. 10. The dependence of the critical current on the normalized temperature [plotted as $[I_c(T)/I_c(10\,\mathrm{K})]^{2/3}$ vs T/T_c in the figures on the left] compared to the temperature dependence of the relaxation rate S in the figures on the right for underdoped TIBCCO (2201) and BiSCCO (2212) disk-shaped films. Note that $I_c(T)$ is dominated by an underdoped GL-like component at low temperatures. A tail close to T_c implies the presence of an unidentified second component (phase).

governed by the nanoscopic phase separation and not by the pinning potential. In fact, this is the nanoscopic phase separation, which is responsible for the spatial variation of the order parameter in a superconductor [see Fig. 1(c)] and, therefore, for the spatial changes in the pinning potential.

There are intriguing similarities between the relaxation effects observed in unirradiated samples and those seen in irradiated YBCO crystals.[14] $S(T)$ at 36 K and 0.5 T for YBCO crystals (irradiated to a dose corresponding to a matching field of 2.4 T) approaches a value of about 0.11 as one would expect for variable-range vortex hopping. However, similar rates of 0.12 at 40 K and 0.14 at 23 K were also found in unirradiated YBCO and BSCCO crystals, respectively.[3,1] This was done during the measurements of remnant magnetization after a field cooling in 500 G, which was applied in a direction parallel to the c axis. In unirradiated YBCO thin films (Figs. 3–5), T_c of an underdoped GL-like phase is correlated with a reduction of S on the high-temperature part of the peak as the temperature is increased. On the other hand, the data for irradiated YBCO in Fig. 1 of Ref. 14, which are plotted as $\log J$ versus temperature, suggest that the crossover in $J(T)$ is associated with the peak in $S(T)$. In order to compare these results with ours shown in Fig. 3–5, we replotted the data of Ref. 14 using a $J^{2/3}$ versus temperature scale [see Fig. 11(a)]. This diagram reveals that the crossover in $J(T)$ occurs on the high-temperature side of the peak in $S(T)$ [see Fig. 11(b)] as found in unirradiated YBCO films. The low $T_c=43$ K and high $T_c=90$ K components in $J(T)$ at 0.5 T are similar to those observed in unirradiated YBCO thin films (Figs. 3–5). They are shown in Fig. 11 (c) as a dashed line for an underdoped GL-like component and as solid triangles for an optimally doped AB-like component. The superposition of these two gives a solid line: a theoretical fit to the experimental data (open circles). The ratio of a GL-like current to an AB-like one at 10 K is about 7. The highest ratio at 10 K observed in YBCO thin films in the present experiments is about 1.5, a factor of 4–5 less than in an irradiated YBCO crystal at 0.5 T.

Figure 12 shows $J_c(T)$ and $S(T)$ for irradiated YBCO film Nos. 1 and 7 in comparison with those for unirradiated films. An irradiation of YBCO No. 1 with 1.4 GeV uranium ions (to a dose corresponding to a matching field of 0.5 T) increases the amount of an optimally doped AB-like phase by about 5% [Fig. 12(b)]. On the other hand, an irradiation of YBCO No. 7 with 1.4 GeV lead ions to the same dose increases the amount of an AB-like phase by about 17% [Fig. 12(c)]. An increase of the amount of the AB-like phase is the only systematic effect of the heavy-ion irradiation. An increase of the amount of the Josephson-like phase has been also observed by Mezzetti *et al.*[29] in YBCO thin films irradiated with 0.25 GeV gold ions. They observed an extension of a plateau seen on the J versus $\log B$ graph to higher fields in irradiated samples. The plateau in the high-current regime has been attributed to the presence of an array of Josephson junctions. Both results imply that irradiation with high-energy heavy ions changes the separation of phases in a superconductor, i.e., decreases the ratio of the critical currents I_c^{GL} (underdoped)/I_c^{AB} (optimally doped) at 10 K in comparison to that observed in the same sample before irradiation. These results show that vortex dynamics is governed by this ratio and not by the columnar defects alone.

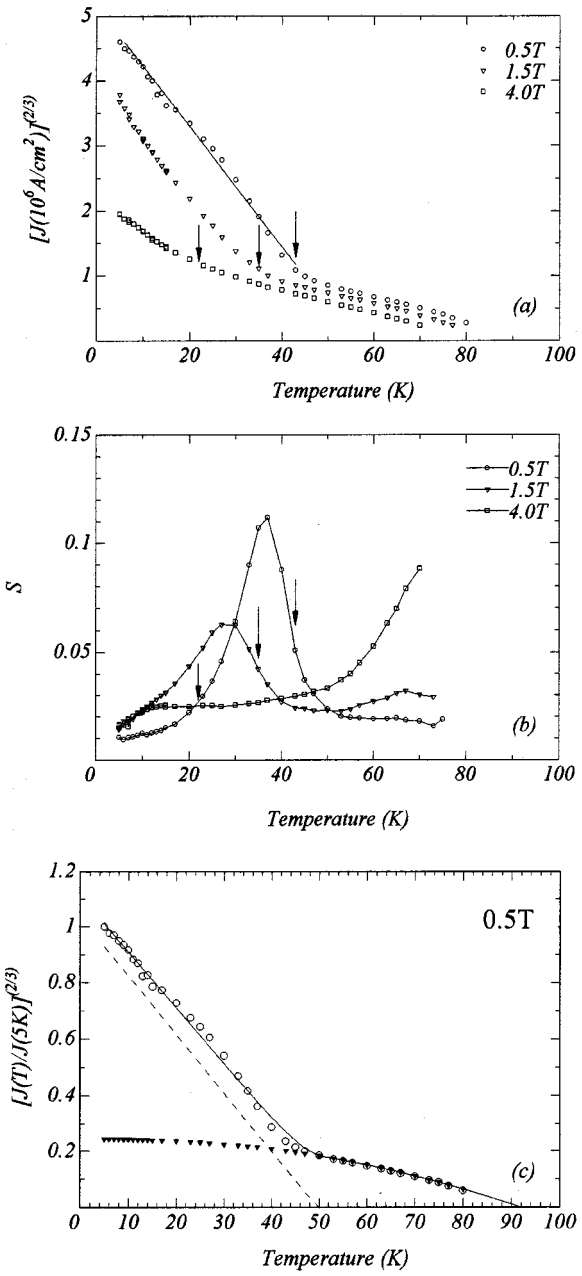

FIG. 11. The data for $J(T)$ [in (a)] and $S(T)$ [in (b)] measured in 1.4 GeV gold-irradiated YBCO single crystal to a dose corresponding to a matching field of 2.4 T [from Thompson *et al.* (Ref. 14)] replotted as $J^{2/3}$ versus temperature. The arrows indicate crossover temperatures in $J(T)$, which correspond to a decrease of S in the peak as the temperature is increased (data obtained by courtesy of J. R. Thompson). (c) The theoretical fit (solid line) to the experimental data (open circles) for $J(T)$ at 0.5 T. The solid line is a superposition of two components to $J(T)$: an AB-like one [solid triangles Clem's model (Ref. 21)] and a GL-like one (dashed line).

Regarding the magnetic relaxation effects in irradiated YBCO single crystals (see Fig. 11), the authors of Ref. 14 have not measured the temperature dependence of J and its time decay in the same sample before irradiation with heavy ions. However, the data by Abulafia *et al.*[30] for $J_c(T)$ in unirradiated YBCO crystals have revealed that $J_c(T)$ has a pure GL-like temperature dependence with $J_c=0$ at about 80 K. Figure 11(c) therefore implies that irradiation introduces

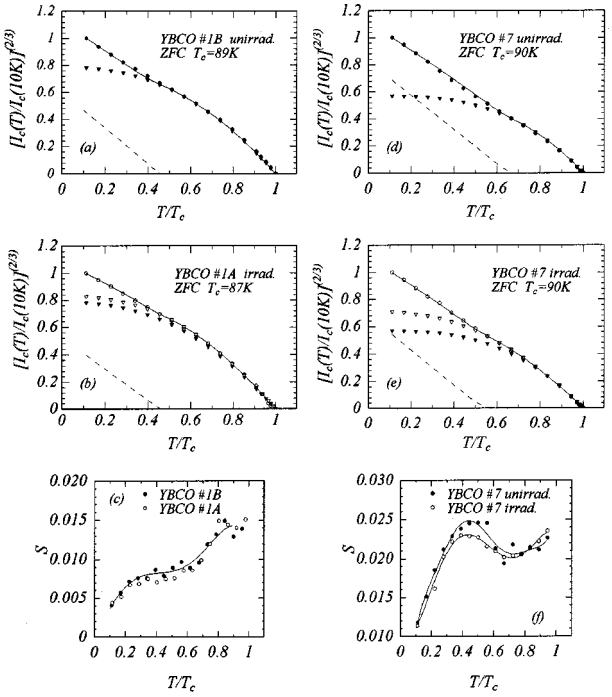

FIG. 12. (a) and (d) $J_c(T)$ for unirradiated films of YBCO No. 1B and YBCO No. 7. (b) and (e) $J_c(T)$ for irradiated films of YBCO No. 1A (with a 1.4 GeV uranium) and YBCO No. 7 (with a 1.4 GeV lead) to a dose corresponding to a matching field of 0.5 T. Solid triangles: the AB-like components of unirradiated samples taken from (a) and (d). Comparison of the AB-like components for irradiated and unirradiated samples suggests an irradiation-induced phase separation. (c) and (f) Corresponding data for $S(T)$ for unirradiated and irradiated YBCO films. Measurement of J_c at 10 K for irradiated YBCO No. 1A revealed an increase of the current density by about 20% but a reduction by about 6% for irradiated YBCO No. 7 in comparison to J_c of unirradiated samples.

an optimally doped AB-like phase (solid triangles) into the YBCO crystals. In a magnetic field of 0.5 T, the ratio of the currents J (underdoped GL-like with $T_c=43$ K) to J (optimally doped AB-like with $T_c=90$ K) at 10 K is approximately 7. According to Fig. 6, this means the relaxation rate S could reach a value of 0.08–0.09, which is 5–6 times higher than the highest rates found by us in YBCO films.

We would like to point out that our studies indicate that the fast relaxation effects can be observed in multiphase superconductors. A proper ratio of at least two phases is required in order to stimulate formation of a magnetic relaxation peak. In a single phase system, either an underdoped one or an optimally doped one, these effects have not been observed.

In fact, the measurements of $J_c(T)$ and $S(T)$ is a good test of a sample's homogeneity. Extensive high-precision x-ray diffraction studies performed by the Naval Research Laboratory[31–33] on YBCO single crystals have shown that the sharpness of the superconducting transition alone is not a good indicator of homogeneity of a superconductor.

V. CONCLUSIONS

The results of this research imply that vortex dynamics (vortex-phase diagrams) could be affected by the nanoscopic

filamentary phase separation of underdoped and optimally doped phases. In YBCO thin films the magnitude of the relaxation rate S at low temperature depends on the relative quantity of underdoped and optimally doped phases in a-b plane nanostructures, as shown schematically in Fig. 1(c). These nanostructures from a ''disordered chessboard'' which can be arranged with an infinite number of possibilities. Our results have shown that the low-temperature peak in $S(T)$ develops when the amount of an underdoped phase in the nanostructures increases at the cost of an optimally doped one. The peak is a characteristic of a superconductor which consists of mixed phases, and it does not appear in samples that contain a single optimally doped or an underdoped phase.

Researchers often assume that their samples (single crystals or thin films) are homogeneous, neglecting the fact that the superconducting order parameter could vary over nanoscopic distances equal to the Ginzburg-Landau coherence length. Nanostructures like those shown in Fig. 1(c) govern the pinning of magnetic vortices, due to the spatial variation of the order parameter.

As mentioned in the Introduction, two peaks in $S(T)$ of remnant magnetization for unirradiated BiSCCO (2212) crystals were investigated by Tuominen *et al.*[1] using the measurements of longitudinal and transverse components of magnetic moment for different orientation angle θ of an applied magnetic field with respect to the c axis. The height of a low-temperature peak was found to decrease and that at a higher temperature (close to T_c) to increase with increasing angle θ. According to our argument, these two peaks could be caused by the presence of two underdoped phases in the sample. For a longitudinal magnetization a decrease in the magnitude of the low-temperature peak with increasing θ suggests phase separation in the a-b planes. An increase in the magnitude of the high-temperature peak with θ, on the other hand, could imply the presence of phase separation along the c axis of the crystal, with layers of an underdoped phase sandwiched between the layers of an optimally doped one.

This work supports ideas of filamentary fragmentation[34] and a fractal dissipative regime[35] in high-T_c superconductors.

ACKNOWLEDGMENTS

We are grateful to Dr. M. Denhoff, Dr. A. Fife, Dr. R. Hughes, Dr. J. Preston, Dr. J. Z. Sun, Dr. J. Talvacchio, and Dr. B. Willemsen for supplying us with high-T_c thin films. This work was supported by a grant from the Natural Sciences and Engineering Council of Canada. The work at SUNY-Buffalo was sponsored by the DOE Division of Materials Sciences, Office of Basic Energy Sciences, under Contract No. DEFG0298ER45719.

*Author to whom correspondence should be addressed. Electronic address: jung@phys.ualberta.ca

†Permanent address: School of Science and Engineering, Alakhawayn University, Ifrane 5300, Morocco.

‡Permanent address: Department of Physics, Boston College, Chestnut Hill, MA 02467.

[1] M. Tuominen, A. M. Goldman, Y. C. Chang, and P. Z. Jiang, Phys. Rev. B **42**, 8740 (1990).

[2] M. Tuominen, Ph.D. thesis, University of Minnesota, 1990.

[3] M. Tuominen, A. M. Goldman, and M. L. Mecartney, Physica C **153-155**, 324 (1988).

[4] C. Keller, H. Küpfer, R. Meier-Hirmer, U. Wiech, V. Selvamanickam, and K. Salama, Cryogenics **30**, 410 (1990).

[5] P. J. Kung, M. P. Maley, M. E. McHenry, J. O. Willis, J. Y. Coulter, M. Murakami, and S. Tanaka, Phys. Rev. B **46**, 6427 (1992).

[6] C. Rossel and P. Chaudhari, Physica C **153-155**, 306 (1988).

[7] S. W. Goodyear, J. S. Satchell, R. G. Humphreys, N. G. Chew, and J. A. Edwards, Physica C **192**, 85 (1992).

[8] M. Tuominen, A. M. Goldman, and M. L. Mecartney, Phys. Rev. B **37**, 548 (1988).

[9] C. Mee, A. I. M. Raie, W. F. Vinen, and C. E. Gough, Phys. Rev. B **43**, 2946 (1991).

[10] L. M. Paulius, C. C. Almasan, and M. B. Maple, Phys. Rev. B **47**, 11 627 (1993).

[11] D. A. Brawner, N. P. Ong, and Z. Z. Wang, Phys. Rev. B **47**, 1156 (1993).

[12] J. R. Thompson, Y. R. Sun, L. Civale, A. P. Malozemoff, M. W. McElfresh, A. D. Marwick, and F. Holtzberg, Phys. Rev. B **47**, 14 440 (1993).

[13] L. Civale, A. D. Marwick, M. W. McElfresh, T. K. Worthington, A. P. Malozemoff, F. Holtzberg, J. R. Thompson, and M. A. Kirk, Phys. Rev. Lett. **65**, 1164 (1990).

[14] J. R. Thompson, L. Krusin-Elbaum, L. Civale, G. Blatter, and C. Feild, Phys. Rev. Lett. **78**, 3181 (1997).

[15] L. Krusin-Elbaum, L. Civale, J. R. Thompson, and C. Feild, Phys. Rev. B **53**, 11 744 (1996).

[16] L. Civale, G. Pasquini, P. Levy, G. Nieva, D. Casa, and H. Lanza, Physica C **263**, 389 (1996).

[17] L. Civale, L. Krusin-Elbaum, J. R. Thompson, R. Wheeler, A. D. Marwick, M. A. Kirk, Y. R. Sun, F. Holtzberg, and C. Feild, Phys. Rev. B **50**, 4102 (1994).

[18] L. Krusin-Elbaum, G. Blatter, J. R. Thompson, D. K. Petrov, R. Wheeler, J. Ullmann, and C. W. Chu, Phys. Rev. Lett. **81**, 3948 (1998).

[19] C. W. Hagen and R. Griessen, Phys. Rev. Lett. **62**, 2857 (1989).

[20] J. Etheridge, Philos. Mag. A **73**, 643 (1996).

[21] J. R. Clem, B. Bumble, S. I. Raider, W. J. Gallagher, and Y. C. Shih, Phys. Rev. B **35**, 6637 (1987).

[22] H. Darhmaoui and J. Jung, Phys. Rev. B **53**, 14 621 (1996).

[23] H. Darhmaoui and J. Jung, Phys. Rev. B **57**, 8009 (1998).

[24] E. C. Jones, D. K. Christen, J. R. Thompson, R. Feenstra, S. Zhu, D. H. Lowndes, J. M. Phillips, M. P. Siegal, and J. D. Budai, Phys. Rev. B **47**, 8986 (1993).

[25] V. Z. Kresin (private communication).

[26] G. Blatter, M. V. Feigelman, V. B. Geshkenbein, A. I. Larkin, and V. M. Vinokur, Rev. Mod. Phys. **66**, 1125 (1994).

[27] J. R. Thompson (private communication).

[28] J. Jung, H. Yan, B. Boyce, J. Skinta, and T. Lemberger (unpublished).

[29] E. Mezzetti, E. Crescio, R. Gerbaldo, G. Ghige, L. Gozzelino, B. Minetti, C. Camerlingo, A. Monaco, G. Cuttone, and A. Rovelli, Phys. Rev. B **60**, 7623 (1999).

[30] Y. Abulafia, A. Shaulov, Y. Wolfus, R. Prozorov, L. Burlachkov,

Y. Yeshurun, D. Majer, E. Zeldov, and V. M. Vinokur, Phys. Rev. Lett. **75**, 2404 (1995).
[31] V. M. Browning, E. F. Skelton, M. S. Osofsky, S. B. Quadri, J. Z. Hu, L. W. Finger, and P. Caubet, Phys. Rev. B **56**, 2860 (1997).
[32] S. B. Quadri, M. S. Osofsky, V. M. Browning, and E. F. Skelton, Appl. Phys. Lett. **68**, 2729 (1996).
[33] E. F. Skelton, S. B. Quadri, M. S. Osofsky, A. R. Drews, P. R. Broussard, J. Z. Hu, L. W. Finger, T. A. Vanderah, D. Kaiser, J. L. Peng, S. M. Anlage, R. L. Greene, and J. Giapintzakis, Proc. SPIE **2516**, 160 (1995).
[34] J. C. Phillips, Proc. SPIE **3481**, 87 (1998).
[35] M. Prester, Phys. Rev. B **60**, 3100 (1999), and references therein.